The International Journal of Advanced Manufacturing Technology (2019) 102:2865–2876
https://doi.org/10.1007/s00170-019-03286-0

ORIGINAL ARTICLE

Inverse identification of Johnson-Cook material constants based on modified chip formation model and iterative gradient search using temperature and force measurements

Jinqiang Ning [1] · Steven Y. Liang [1]

Received: 4 September 2018 / Accepted: 2 January 2019 / Published online: 7 February 2019

Abstract
This paper presents an improved inverse identification method for Johnson-Cook model constants (J-C constants) using force and temperature data. Nowadays, J-C constants are identified by either experimental approaches with the complex and costly system, numerical approaches with high computational cost, or analytical approaches with available material properties. The previous model is developed based on a modified chip formation model and an exhaustive search method using temperature and force measurements. The current model is improved by replacing the exhaustive search method with an iterative gradient search method based on the Kalman filter algorithm. The modified chip formation model is used to predict machining forces. The iterative gradient search method is used to determine the J-C constants when the difference between predicted forces and experimental forces reached an acceptable low value. AISI 1045 steel and Al6082-T6 aluminum are chosen to test the proposed methodology. The determined J-C constants are validated by comparing to the documented values in the literature, which were obtained from Split-Hopkinson Pressure Bar tests and validated in published works. Good agreements are observed between identified J-C constants and documented values with an improved computational efficiency. The cutting temperatures are used as inputs in the modified chip formation model. Therefore, the workpiece material properties are not required to predict temperatures and forces, and thus are not required for determining J-C constants. Considering the modified chip formation model using temperatures as inputs, and the effective iterative gradient search method, this method has advantages of less mathematical complexity and high computational efficiency.

Keywords Inverse identification · Johnson-Cook model constants · Modified chip formation model · Iterative gradient search · Kalman filter

1 Introduction

Constitutive relation describes materials behavior under different loading conditions. It is needed in the modeling of force, temperature, and residual stress in the machining process [1–3]. Johnson-Cook model (J-C model) is one of the constitutive models widely used in analytical modeling of force, temperature, and residual stress because it is effective, simple, and easy-to-use [4].

In the past, researchers have developed different approaches to identify the J-C model constants (J-C constants) for various materials. The developed approaches can be broadly classified into experimental approach, numerical approach, and analytical approach. The experimental approaches used quasi-static tests at different temperatures and dynamic tests at different strain rates to identify J-C constants [5–8]. Split-Hopkinson pressure bar (SHPB) test is a typical experimental approach for identifying material constitutive model parameters [9]. The numerical approaches used finite element analysis (FEA) to simulate the machining process. Chip morphology, machining force, temperature, and residual stress from the simulation were often compared to

✉ Jinqiang Ning
jinqiangning@gatech.eduand

Steven Y. Liang
steven.liang@me.gatech.edu

[1] George W. Woodruff School of Mechanical Engineering, Georgia Institute of Technology, 801 Ferst Drive, Atlanta, GA 30332-0405, USA

experimental measurements to identify J-C constants [10–12]. Analytical approaches were also developed to identify J-C constants. Tounsi et al. developed an analytical approach based on strain, stress, and temperature in the orthogonal machining with a least-square approximation technique to identify J-C constants [13]. Quick stop cutting tests and microstructure analyses were needed to measure those physical quantities for the identification. Multiple cutting tests were needed for each identification of J-C constants. Özel and Karpat developed another analytical approach to identify J-C constants using particle swarm optimization (PSO) and experimental measurements of strain, stress, and temperature from SHPB compression tests [14]. Naik P. and Naik A. developed an approach based on chip formation model and exhaustive search method to inversely identify the J-C constants using cutting condition parameters and material properties of the workpiece [15]. Denkena et al. developed another inverse identification methodology based on PSO and chip formation model using the cutting condition parameters and material properties of the workpiece [16]. Ning and Liang developed an analytical model based on a modified chip formation model to identify J-C constants with force and temperature measurements [17]. Ning et al. developed another analytical model based on chip formation model and an iterative gradient search method to identify J-C constants with improved computational efficiency [18]. The former model requires force and temperature measurements as inputs; the latter requires force measurements and material properties as inputs.

Although the aforementioned approaches have made considerable progress in identifying J-C constants, the identification of J-C constants remained difficult and challenging due to the high experimental complexity, high mathematical complexity, and low computational efficiency. The experimental approaches require complex and costly system such as SHPB tests. The numerical approaches have high computational cost and a large number of input parameters such as experimental measurements and material properties, which must be obtained from extensive experimental works and material property tests. The approaches developed by Tounsi, Naik, and Denkena need material properties of the workpiece to identify the J-C constants. Özel's approach needs experimental measurements from complex and costly SHPB tests. Naik's approach and Ning's former approach use exhaustive search method to identify J-C constants, which prevents an optimized computational efficiency. Ning's latter approach employs an iterative gradient search method to further improve computation efficiency but needs material properties of the workpiece.

In this paper, the authors present an analytical approach based on a modified chip formation model and an iterative gradient search method using Kalman filter algorithm to inversely identify the J-C constants. Machining forces are predicted with the modified chip formation model using cutting condition, cutting temperatures, and a set of initial J-C constants as inputs. Material properties are not needed in the prediction. The iterative gradient search method is employed to determine the J-C constants when the difference between the predicted forces and experimental forces reaches an acceptable low value. The use of temperature measurements as inputs in the modified chip formation model reduces mathematical complexity and thus improves the computational efficiency. The use of iterative gradient search method also improves the computational efficiency. AISI 1045 steel and AL 6082-T6 aluminum are chosen to test the proposed approach. The identified J-C constants for each material are validated with the documented values obtained from SHPB experiments [19, 20].

2 Material and methodology

2.1 Johnson-Cook flow stress model

J-C model is a semi-empirical constitutive model that predicts material flow stress at high strains, high strain rates, and high temperatures. The J-C model is expressed as

$$\sigma = (A + B\varepsilon^n)\left[1 + C\ln\left(\frac{\dot{\varepsilon}}{\dot{\varepsilon}_0}\right)\right]\left[1-\left(\frac{T-T_r}{T_m-T_r}\right)^m\right] \quad (1)$$

where A, B, c, n, and m are the five model constants. A is the yield stress, B is the strength coefficient, C is the strain rate coefficient, n is the strain hardening coefficient, and m is the thermal softening coefficient. Other terms are explained in the

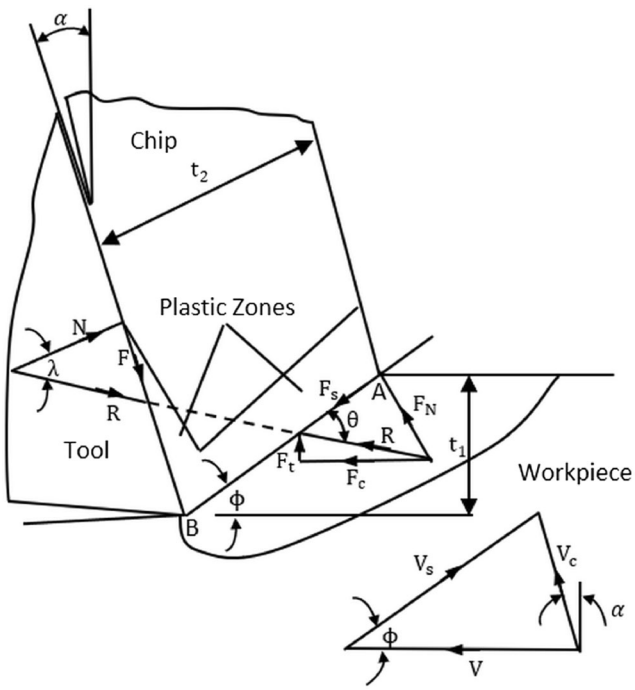

Fig. 1 Chip formation model in orthogonal cutting [25]

following. σ is the material flow stress, ε is the plastic strain, $\dot{\varepsilon}$ is the plastic strain rate, $\dot{\varepsilon_0}$ is the reference plastic strain rate, T is the temperature of the workpiece material, T_r is the reference temperature, and T_m is the material melting temperature. J-C model is widely used in predicting material behavior and failure under various strain and temperature conditions [21], and also in analytical modeling of force, temperature, and residual stress in machining process because it is effective, simple, and easy-to-use [22, 23].

2.2 Modified chip formation model

A chip formation model, as originally proposed by Oxley [24], has been widely referenced for the prediction of machining force, temperature distribution, and residual stress with the material properties of the workpiece, and cutting condition parameters including cutting speed, depth of cut, and width of cut in orthogonal machining. This paper employed a modified chip formation model using temperature measurements rather than temperature predictions based on material properties and cutting condition to predict machining forces because the properties of workpiece were commonly required to predict the temperature, but they were often unknown. The modified chip formation model did not require the material properties (thermal properties, mechanical properties, and physical properties) of the workpiece to predict machining forces, which reduced the workload of finding the material properties, reduced the mathematical complexity of the model, and resulted in an improved computational efficiency. The measurements of average temperatures at the primary shear zone (PSZ) and at the tool-chip interface (secondary shear zone or SSZ) have been reported in the literature with infrared (IR) camera system and intrinsic thermocouple technique respectively. The techniques of temperature measurements will be discussed in detail in Section 2.4. The average temperature at PSZ and the average temperature at SSZ were estimated based on the assumptions used in the modified chip formation model. The assumptions were (1) a perfectly sharp cutting tool under plain strain and steady-state condition, (2) straight-line shape of PSZ near the center of the shear plane field, and (3) uniform strain and uniform temperature in the PSZ and the

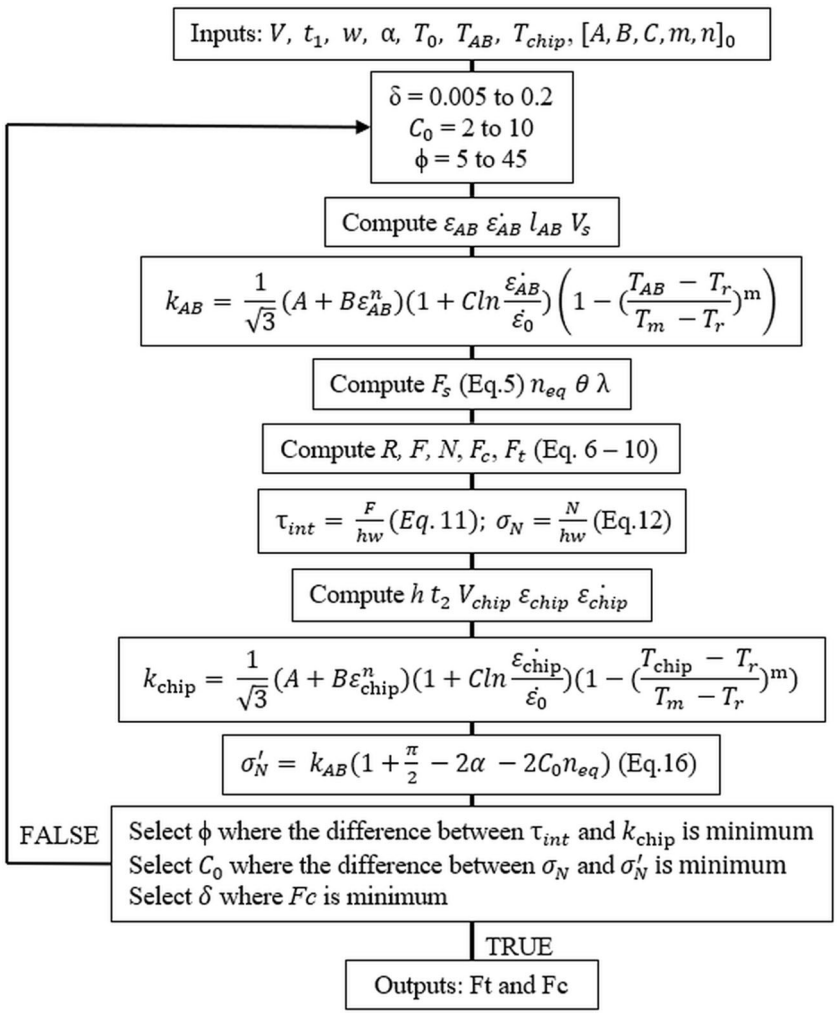

Fig. 2 The algorithm of the modified chip formation model for the prediction of machining force

SSZ. The chip formation model in orthogonal cutting configuration is illustrated as in Fig. 1, where α is the rake angle, ϕ is the shear angle, λ is the average friction angle at the tool-chip interface, and θ is the angle between resultant cutting force R and primary shear zone AB. t_1t_2 are the depth of cut and the chip thickness respectively. V, V_s, V_c are the cutting velocity, shear velocity, and chip velocity respectively. w is the width of cut that is not shown.

As shown in Fig. 2, the cutting condition parameters including cutting speed, width of cut, depth of cut, tool face rake angle, and process variables including the average temperature at PSZ and the average temperature at SSZ are given as inputs. The F_c and F_t are computed with a determined shear angle (ϕ), and two strain rate constants (δ, C_0). As shown in Fig. 3, δ is the ratio of the thickness of SSZ to chip thickness ($\Delta s_1/t_2$) and C_0 is the ratio of shear plane length to the thickness of the PSZ ($l/\Delta s_2$).

The shear flow stress on shear plane AB (k_{AB}) with von Mises criterion is expressed as

$$k_{AB} = \frac{1}{\sqrt{3}}\left(A + B\varepsilon_{AB}^{n}\right)\left(1 + C\ln\frac{\dot{\varepsilon}_{AB}}{\dot{\varepsilon}_0}\right)\left[1-\left(\frac{T_{AB}-T_r}{T_m-T_r}\right)^{m}\right] \tag{2}$$

where strain (ε_{AB}) and strain rate ($\dot{\varepsilon}_{AB}$) on the shear plane AB with von Mises yield criterion are

$$\varepsilon_{AB} = \frac{\gamma_{AB}}{\sqrt{3}} = \frac{\cos\alpha}{2\sqrt{3}\sin\phi\cos(\phi-\alpha)} \tag{3}$$

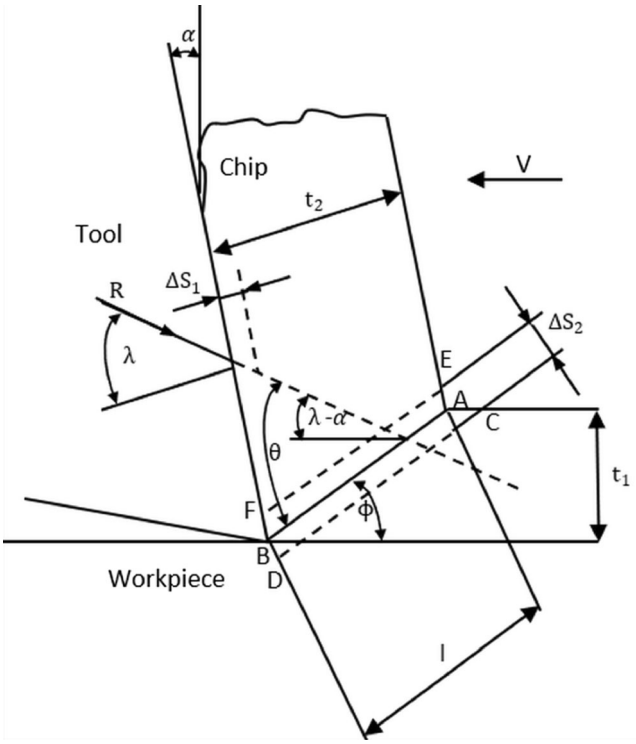

Fig. 3 Parallel-sided shear zone model [24]

$$\dot{\varepsilon}_{AB} = \frac{\dot{\gamma}_{AB}}{\sqrt{3}} = C_0\frac{V_s}{\sqrt{3}l_{AB}} \tag{4}$$

The shear force (F_s) is calculated as

$$F_s = k_{AB}l_{AB}w \tag{5}$$

The resultant force (R), the shear force (F), and the normal force (N) at the tool-chip interface, and the cutting force (F_c) and the thrust force (F_t) are calculated as

$$R = \frac{F_s}{\cos\theta} \tag{6}$$

$$F = R\sin\lambda \tag{7}$$

$$N = R\cos\lambda \tag{8}$$

$$F_c = R\cos(\lambda-\alpha) \tag{9}$$

$$F_t = R\sin(\lambda-\alpha) \tag{10}$$

The shear stress (τ_{int}) and normal stress (σ_N) in the SSZ using chip formation model are calculated as

$$\tau_{\text{int}} = \frac{F}{hw} \tag{11}$$

$$\sigma_N = \frac{N}{hw} \tag{12}$$

The shear stress (k_{chip}) and the normal stress (σ_N') in the SSZ are also calculated using J-C model as

$$k_{\text{chip}} = \frac{1}{\sqrt{3}}\left(A + B\varepsilon_{\text{int}}^{n}\right)\left(1 + C\ln\frac{\dot{\varepsilon}_{\text{int}}}{\dot{\varepsilon}_0}\right)\left[1-\left(\frac{T_{\text{int}}-T_r}{T_m-T_r}\right)^{m}\right] \tag{13}$$

where strain (ε_{int}) and strain rate ($\dot{\varepsilon}_{int}$) on the tool-chip interface with von Mises yield criterion are

$$\varepsilon_{\text{chip}} = \frac{\gamma_{\text{int}}}{\sqrt{3}} = 2\varepsilon_{AB} + \frac{h}{2\sqrt{3}\delta t_2} \tag{14}$$

$$\dot{\varepsilon}_{\text{chip}} = \frac{\dot{\gamma}_{\text{int}}}{\sqrt{3}} = \frac{V_c}{\sqrt{3}\delta t_2} \tag{15}$$

$$\sigma_N' = k_{AB}\left(1 + \frac{\pi}{2} - 2\alpha - 2C_0n_{\text{eq}}\right) \tag{16}$$

Other variables including contact length on the tool-chip interface (h), length of primary shear the zone (l_{AB}), chip thickness (t_2), angles (θ, λ), and velocities (V_s, V_{chip}) are calculated by the equations listed in the Appendix.

2.3 Iterative gradient search method

Kalman filter [26] is a computational gradient search method that has been used in many applications of root finding and

inverse analysis. The algorithm is employed here with the modified chip formation model to identify J-C constants. This method only needs experimental measurements from one orthogonal cutting to identify J-C constants. The Kalman filter is given in a general form as

$$x_t = x_{t-1} + K_t\left(d_{\exp} - d_{t-1}\right) \tag{17}$$

where $x_t = (A_t\ B_t\ \ C_t\ m_t\ n_t\ T_{mt})^T$ and A, B, C, m, n are the J-C constants, and T_m is the melting temperature of workpiece material. The initial values of x are $x_0 = (A_0\ B_0\ \ C_0\ m_0\ n_0\ T_{m0})^T$.

$d_{\exp}$ and d_{t-1} are expressed as

$$d_{\exp} = \left(F_c^{\exp}\ F_t^{\exp}\right)^T \tag{18}$$

$$d_{t-1} = \left(F_c^{t-1}\ F_t^{t-1}\right) \tag{19}$$

where F_c and F_t are cutting force and thrust force respectively in orthogonal cutting.

The Kalman gain matrix K_t is expressed with a covariance matrix P_t and error covariance matrix R_t. They are expressed as

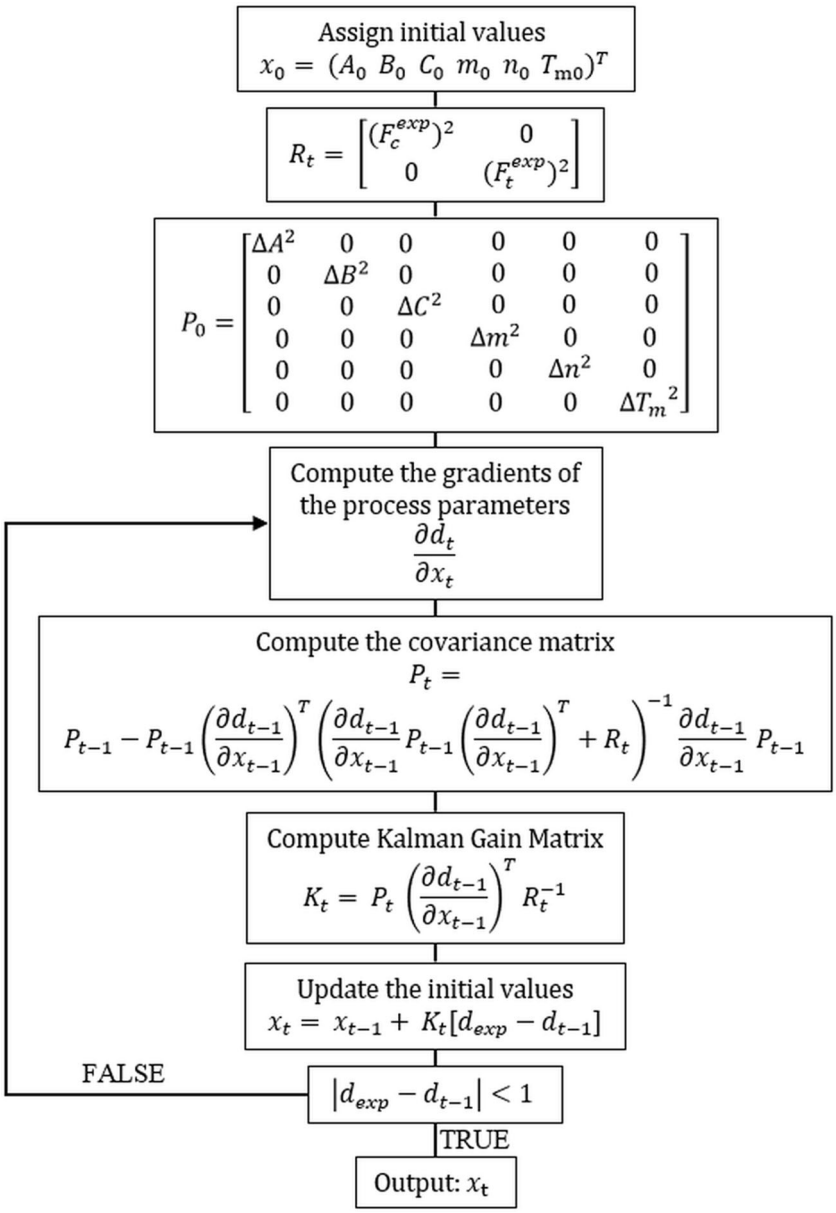

Fig. 4 The algorithm of an iterative gradient search method based on Kalman filter for identification of J-C constants

$$K_t = P_t \left(\frac{\partial d_{t-1}}{\partial x_{t-1}}\right)^T R_t^{-1} \tag{20}$$

$$P_t = P_{t-1} - P_{t-1}\left(\frac{\partial d_{t-1}}{\partial x_{t-1}}\right)^T \left[\frac{\partial d_{t-1}}{\partial x_{t-1}} P_{t-1} \left(\frac{\partial d_{t-1}}{\partial x_{t-1}}\right)^T + R_t\right]^{-1} \frac{\partial d_{t-1}}{\partial x_{t-1}} P_{t-1} \tag{21}$$

The initial values of P_0 and R_t are expressed as

$$P_0 = \begin{bmatrix} \Delta A^2 & 0 & 0 & 0 & 0 & 0 \\ 0 & \Delta B^2 & 0 & 0 & 0 & 0 \\ 0 & 0 & \Delta C^2 & 0 & 0 & 0 \\ 0 & 0 & 0 & \Delta m^2 & 0 & 0 \\ 0 & 0 & 0 & 0 & \Delta n^2 & 0 \\ 0 & 0 & 0 & 0 & 0 & \Delta T_m{}^2 \end{bmatrix} \tag{22}$$

$$R_t = \begin{bmatrix} \left(F_c^{\exp}\right)^2 & 0 \\ 0 & \left(F_t^{\exp}\right)^2 \end{bmatrix} \tag{23}$$

where ΔA to ΔT_m are the estimated deviations of unknown J-C constants and melting temperature of workpiece material.

The J-C constants and the melting temperature of workpiece material are identified with Kalman filter as shown in Fig. 4. The assigned initial values X_0 in the Kalman filter are determined based on the least calibration error in a small number of iterations. The calibration error is calculated as Error $= \left(\mathrm{ABS}\left(F_c^P - F_c^E\right) + ABS\left(F_t^P - F_t^E\right)\right)/\left(F_c^E + F_t^E\right)$ where ABS, $^{\mathrm{P}}$, $^{\mathrm{E}}$ represent absolute value, predicted value, and experimental value respectively. The J-C model constants were determined when the difference between predicted forces and experimental forces is minimal.

2.4 Force and temperature measurements

Machining force and temperature are adopted from literature [27–29], in which orthogonal cutting tests were conducted under various cutting conditions. Machining forces were measured using a three-axis piezoelectric dynamometer [27]. Average temperatures at the PSZ and the SSZ were measured using an IR camera and tool-work thermocouple (intrinsic thermocouple) respectively [28, 29]. This work focuses on the identification methodology of J-C constants. The techniques of temperature measurements are briefly explained in the following.

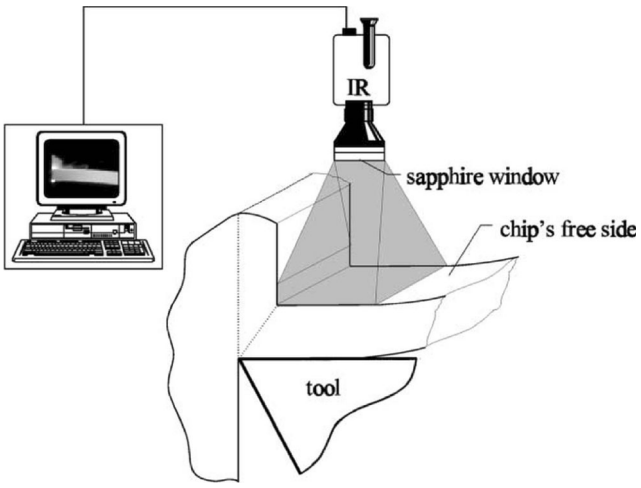

Fig. 5 Schematic view of temperature measurements with IR camera on chip's free size in orthogonal cutting [30]

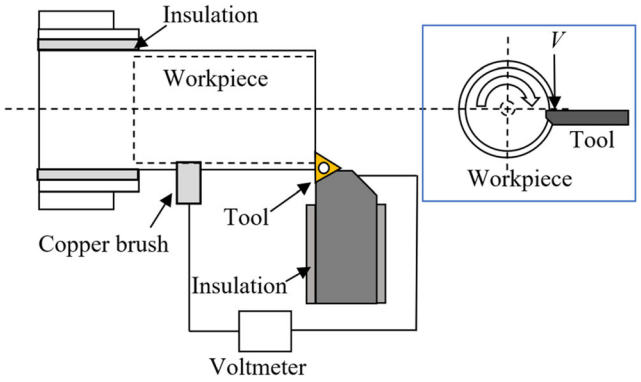

Fig. 6 Schematic view of temperature measurements at the tool-chip interface using intrinsic thermocouple technique [31]

The temperature in the PSZ was measured using an IR camera with spatial resolution around 0.35 mm [30]. The IR camera was placed straight above the rake face of the tool to measure the temperature on chip's free side as shown in Fig. 5. Measurement with each cutting condition was made at least in triplicate. The temperature at cutting edge was discernable and considered as the temperature in the PSZ once it has become stable.

The temperature in the SSZ was measured using the intrinsic thermocouple method [31], in which the tool and workpiece were connected by lead wires to form a closed circuit. The contact area between the tool and the workpiece formed a hot junction; the remote section of the tool and the workpiece formed a cold junction. A copper brush was used to maintain connection during machining. A schematic view of the intrinsic thermocouple in machining is illustrated in Fig. 6. This method is one of the most robust and reliable methods for measuring the average temperature at the tool-chip interface despite the shortcomings of ignoring other bi-conductor interface and the fluctuation of contact area [27].

Table 1 J-C constants obtained from SHPB tests ($\dot{\varepsilon} = 1, T_0 = 25^{\circ}C$)

Material	A (MPa)	B (MPa)	C	m	n	T_m (°C)
AISI 1045 [19]	553.1	600.8	0.0134	1	0.234	1460
AL6082-T6 [20]	250	243.6	0.00747	1.31	0.17	582

Table 2 Cutting conditions, force, and temperature measurements for AISI 1045 steel and AL 6082-T6 aluminum

Material	Test	t_0 (mm)	w (mm)	α (degs)	V (m/s)	T_{AB} (°C)	T_{int} (°C)	Fc (N)	Ft (N)
AISI 1045	1	0.15	1.6	5	3.33	313.12	815.74	583	402
[28]	2	0.3	1.6	− 7	3.33	383.1	992.44	1125	740
	3	0.3	1.6	5	3.33	300.77	941.15	976	493
Material	Test	t_0 (mm)	w (mm)	α (degs)	V (m/s)	T_{AB} (°C)	T_{int} (°C)	Fc (N)	Ft (N)
AL6082-T6	1	0.4	3	8	4	205	464	795	300
[29]	2	0.2	3	8	6	188	493	456	204
	3	0.4	3	8	6	198	508	768	276

Table 3 Identified J-C constants for AISI 1045 steel and AL 6082-T6 aluminum and calibration error

Material	Test	A (MPa)	B (MPa)	C	m	n	T_m (°C)	Error (%)
AISI 1045	Initial	500	500	0.01	1	0.2	1500	
	1	493.93	523.82	0.010	1.025	0.203	1574.33	1.14
	2	623.64	456.72	0.009	1.029	0.185	1561.42	3.16
	3	499.02	500.91	0.011	1.106	0.217	1582.72	4.12
AL 6082-T6	Initial	200	200	0.01	1	0.1	600	
	1	258.30	253.72	0.010	1.238	0.100	786.27	6.26
	2	237.77	238.53	0.012	1.278	0.109	833.03	9.98
	3	225.60	229.32	0.011	1.139	0.106	875.09	6.12

Table 4 Other predicted variables for AISI 1045 steel and AL 6082-T6 aluminum

Material	Test	ϕ (degs)	t_2 (mm)	Material	Test	ϕ (degs)	t_2 (mm)
AISI 1045	1	17.31	0.49	AL 6082-T6	2	29.62	0.38
	2	21.41	0.72		3	31.67	0.70
	3	22.44	0.75		1	29.62	0.75

2.5 Validation

J-C constants are determined with the modified chip formation model and the iterative gradient search method as discussed in Sections 2.2 and 2.3. AISI 1045 steel and AL 6082-T6 aluminum are chosen to test the presented method. The identified J-C constants are validated by comparing to the model constants

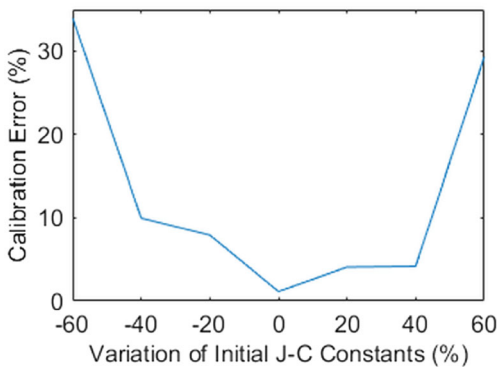

Fig. 7 The sensitivity of initial J-C constants for AISI 1045 steel with test 1 in 50 iterations

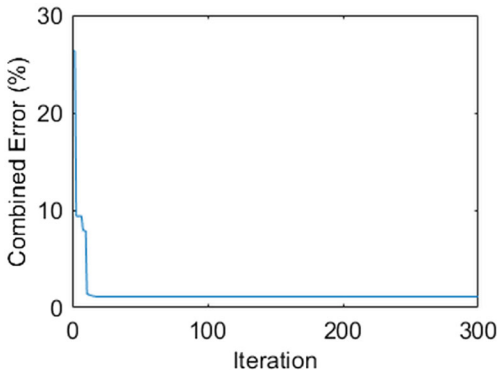

Fig. 8 Calibration errors in determining the J-C constants of AISI 1045 steel with test 1 in 300 iterations

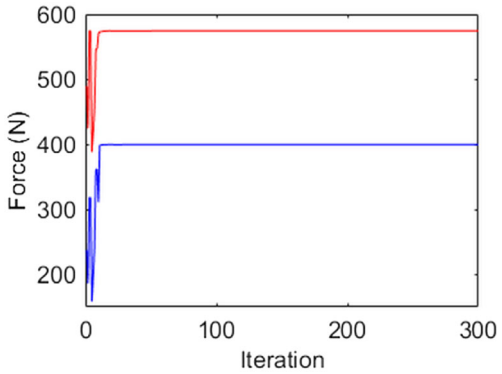

Fig. 9 Predicted forces in determining the J-C constants of AISI 1045 steel with test 1 in 300 iterations. Red line and blue line represent predicted cutting forces and predicted thrust forces respectively

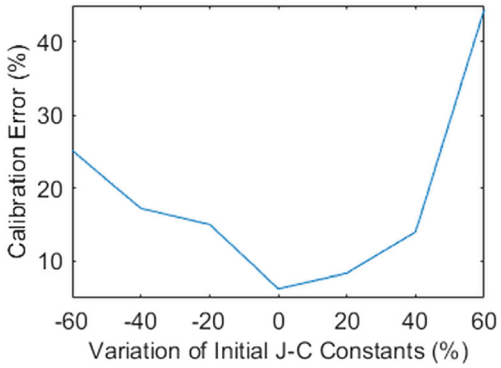

Fig. 11 Sensitivity study of initial J-C constants for AL 6082-T6 aluminum with test 1

documented in the literature. The documented J-C constants were obtained from SHPB tests conducted at strain ranges of 0.05 to 0.2, strain rate of 7500 1/s, and temperature ranges of 35 to 625 °C for AISI 1045 steel [19] and for Al 6082-T6 aluminum [20]. In addition, the documented J-C constants have been validated in analytical modeling of machining process in the literature [29, 32]. The J-C constants and melting temperature of AISI 1045 steel and Al6082-T6 aluminum are given in Table 1.

3 Results and discussion

To test the proposed methodology, J-C constants of AISI 1045 steel and AL 6082-T6 aluminum were determined with temperature and force measurements from multiple orthogonal cutting tests. Inputs including variables of cutting condition, cutting forces, and cutting temperatures are given in Table 2. J-C constants were determined under various cutting conditions. The identified J-C constants and corresponding calibration error with each cutting test are given in Table 3. Other predicted variables are given in Table 4.

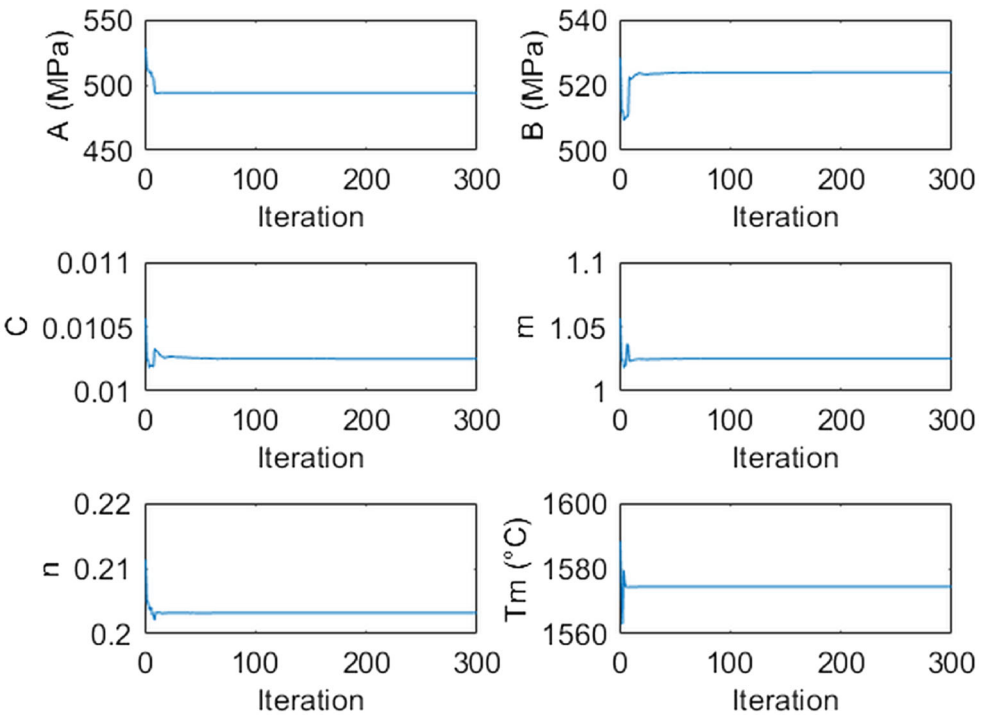

Fig. 10 Convergent patterns of predicted J-C model constants and melting temperature of AISI 1045 steel with test 1 in 300 iterations

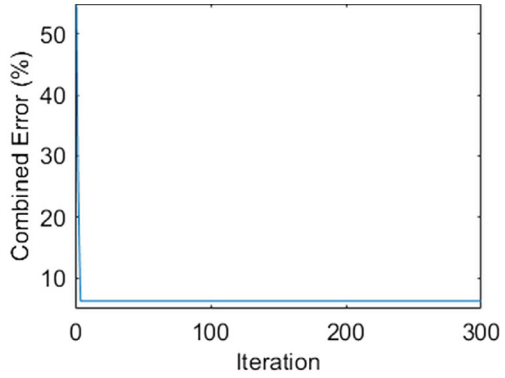

Fig. 12 Calibration errors in determining the J-C constants of AL 6082-T6 aluminum with test 1 in 300 iterations

For AISI 1045 steel, the initial J-C constants were determined based on the least calibration error in a small number of iterations. The sensitivity of initial J-C constants was investigated with the calibration errors by varying each initial J-C constant at the same amount up to 60% as shown in Fig. 7. The least calibration error was observed with the chosen initial J-C constants for AISI 1045 steel as in Table 3. The calibration errors and predicted forces in the identification of the J-C constants of AISI 1045 steel under test 1 cutting condition are shown in Figs. 8 and 9 respectively. A decreasing trend for calibration errors was observed in a small number of iterations. The calibration errors became stable at an acceptable low value. Convergence of predicted forces was observed in a number of iterations. The convergent patterns of each J-C constants in the identification are shown in Fig. 10.

For AL 6082-T6 aluminum, the same method was used to identify J-C constants. The sensitivity of initial J-C constants in the determination is shown in Fig. 11. The least calibration error was observed with chosen initial J-C constants for AL 6082-T6 as in Table 3. The calibration errors, predicted forces, and convergent patterns of each J-C constant in the identification with test 1 are shown in Figs. 12, 13, and 14 respectively.

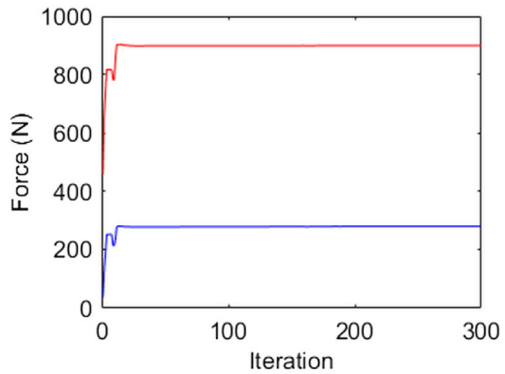

Fig. 13 Predicted forces in the determination of J-C constants of AL 6082-T6 aluminum with test 1 in 300 iterations. Red line and blue line represent predicted cutting forces and predicted thrust forces respectively

With initial J-C constants remaining the same for each material, the J-C constants were identified with more cutting experiments for AISI 1045 steel and AL 6082-T6 aluminum individually. The predicted J-C constants and corresponding error of identification with each test are given in Table 3. The calibration errors for the identifications with all tests are less than 10%. The predicted J-C constants from three cutting experiments were then validated to the documented J-C constants from SHPB tests. As shown in Fig. 15, good agreements between predicted J-C constants and J-C constants from SHPB tests were observed for AISI 1045 steel and AL 6082-T6 aluminum. The deviations between identified J-C constants and J-C constants from SHPB tests were caused by the accuracy of the input cutting force and cutting temperature, and the assumptions made for the modified chip formation model in orthogonal cutting. Moreover, the computational time for each identification of J-C constants with a personal computer running at 2.8 GHz was less than 5 min. For comparison, the computational time for each identification using the previous model without the iterative gradient search method cost a few hours [17].

4 Conclusion

J-C model is widely used in analytical modeling of force, temperature and residual stress in the machining process. This paper presents an effective and efficient analytical approach to inversely identify J-C constants based on a modified chip formation model and an iterative gradient searching method using Kalman filter algorithm with force and temperature measurements in orthogonal machining. Temperature measurements were adopted from literature and used in the modified chip formation model to predict machining forces. The J-C constants were identified when the difference between predicted forces and the experimental forces was minimal. The proposed method requires only one orthogonal cutting experiment with measurements of force and temperature to determine the J-C constants of workpiece material. The material properties of the workpiece are not required for the identification of J-C constants. Good agreements were observed between identified J-C

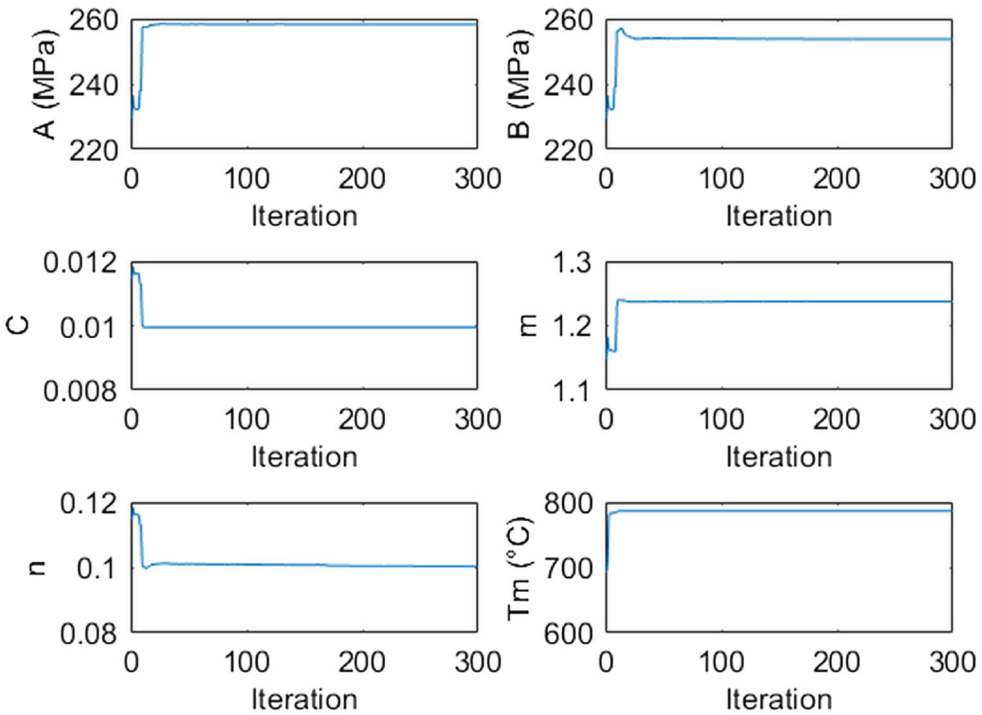

Fig. 14 Convergent patterns of predicted JC model constants and melting temperature of AL 6082-T6 aluminum in 300 iterations

constants and documented values obtained from SHPB tests for AISI 1045 steel and AL 6082-T6 aluminum. In this light fact of the simple orthogonal cutting test, modified chip formation model without using material properties, efficient gradient search method, the proposed method had advantages of less experimental complexity and less mathematical complexity, and high computational efficiency.

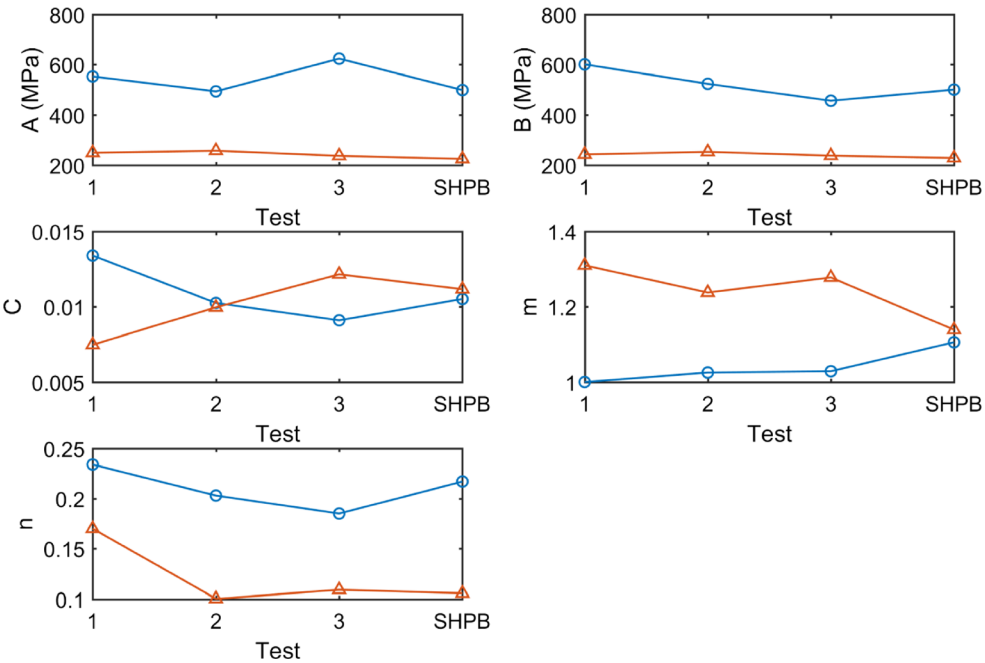

Fig. 15 Identified J-C constants from different cutting tests and documented J-C constants from SHPB tests for AISI 1045 steel and AL 6082-T6 aluminum. 1, 2, and 3 denote the experimental tests used for the identification of J-C constants. SHPB denotes the documented values from SHPB tests for validation purpose. The blue line and red line represent the corresponding values of J-C constant for AISI 1045 steel and AL 6082-T6 aluminum respectively

Funding information This work was supported by the US National Science Foundation under Grant CMMI-1404827.

Appendix

The tool-chip contact length (h) at the tool-chip interface is expressed as

$$h = \frac{t_1 \sin\theta}{\cos\lambda \sin\phi} \left\{ 1 + \frac{C_0 n_{eq}}{3\left[1 + 2\left(\frac{\pi}{4} - \phi\right) - C_0 n_{eq}\right]} \right\} \tag{23}$$

The length of the shear zone (l_{AB}) is calculated based on the orthogonal cutting geometry as

$$l_{AB} = \frac{t_1}{\sin\phi} \tag{24}$$

The angle between the resultant force and primary shear zone AB (θ) and friction angle at the ool-chip interface (λ) in orthogonal cutting are

$$\theta = \arctan\left[1 + 2\left(\frac{\pi}{4} - \phi\right) - C_0 n_{\text{eq}}\right] \tag{25}$$

where strain hardening constant (n_{eq}) is expressed as

$$n_{\text{eq}} = \frac{nB\varepsilon_{AB}^{n}}{\left(A + B\varepsilon_{AB}^{n}\right)} \tag{26}$$

$$\lambda = \theta - \phi + \alpha \tag{27}$$

The shear velocity (V_s) and chip velocity (V_c) are calculates as

$$V_s = \frac{V\cos\alpha}{\cos(\phi - \alpha)} \tag{28}$$

$$V_c = \frac{V\sin\phi}{\cos(\phi - \alpha)} \tag{29}$$

References

1. Ning J, Liang SY (2018) Prediction of temperature distribution in orthogonal machining based on the mechanics of the cutting process using a constitutive model. J Manuf Mater Process 2(2):37. https://doi.org/10.3390/jmmp2020037
2. Ning J, Liang SY (2018) Evaluation of an analytical model in the prediction of machining temperature of AISI 1045 steel and AISI 4340 steel. J Manuf Mater Process 2(4):74. https://doi.org/10.3390/jmmp2040074
3. Ning J, Nguyen V, Liang SY (2018) Analytical modeling of machining forces of ultra-fine-grained titanium. Int J Adv Manuf Technol:1–10. https://doi.org/10.1007/s00170-018-2889-6
4. Johnson GR, Cook WH (1985) Fracture characteristics of three metals subjected to various strains, strain rates, temperatures and pressures. Eng Fract Mech 21(1):31–48. https://doi.org/10.1016/0013-7944(85)90052-9
5. Majzoobi GH, Freshteh-Saniee F, Khosroshahi SF, Mohammadloo HB (2010) Determination of materials parameters under dynamic loading. Part I: experiments and simulations. Comput Mater Sci 49(2):192–200. https://doi.org/10.1016/j.commatsci.2010.03.054
6. Dorogoy A, Rittel D (2009) Determination of the Johnson–Cook material parameters using the SCS specimen. Exp Mech 49(6):881–885. https://doi.org/10.1007/s11340-008-9201-x
7. Khan AS, Suh YS, Kazmi R (2004) Quasi-static and dynamic loading responses and constitutive modeling of titanium alloys. Int J Plast 20(12):2233–2248. https://doi.org/10.1016/j.ijplas.2003.06.005
8. Milani AS, Dabboussi W, Nemes JA, Abeyaratne RC (2009) An improved multi-objective identification of Johnson–Cook material parameters. Int J Impact Eng 36(2):294–302. https://doi.org/10.1016/j.ijimpeng.2008.02.003
9. Kolsky H (1949) An investigation of the mechanical properties of materials at very high rates of loading. Proc Phys Soc London Sect B 62(11):676–700. https://doi.org/10.1088/0370-1301/62/11/302
10. Shrot A, Bäker M (2012) Determination of Johnson–Cook parameters from machining simulations. Comput Mater Sci 52(1):298–304. https://doi.org/10.1016/j.commatsci.2011.07.035
11. Umbrello D, M'saoubi R, Outeiro JC (2017) The influence of Johnson–Cook material constants on finite element simulation of machining of AISI 316L steel. Int J Mach Tools Manuf 47(3–4):462–470. https://doi.org/10.1016/j.ijmachtools.2006.06.006
12. Agmell M, Ahadi A, Ståhl JE (2014) Identification of plasticity constants from orthogonal cutting and inverse analysis. Mech Mater 77:43–51. https://doi.org/10.1016/j.mechmat.2014.07.005
13. Tounsi N, Vincenti J, Otho A, Elbestawi MA (2002) From the basic mechanics of orthogonal metal cutting toward the identification of the constitutive equation. Int J Mach Tools Manuf 42(12):1373–1383. https://doi.org/10.1016/S0890-6955(02)00046-9
14. Özel T, Karpat Y (2007) Identification of constitutive material model parameters for high-strain rate metal cutting conditions using evolutionary computational algorithms. Mater Manuf Process 22(5):659–667. https://doi.org/10.1080/10426910701323631
15. Naik P, Naik A (2015) Determination of flow stress constants by Oxley's theory. International Journal of Latest Technology in Engineering, Management & Applied Science 4(10):110–116 DOI is unavailable
16. Denkena B, Grove T, Dittrich MA, Niederwestberg D, Lahres M (2015) Inverse determination of constitutive equations and cutting force modelling for complex tools using Oxley's predictive machining theory. Procedia CIRP 31:405–410. https://doi.org/10.1016/j.procir.2015.03.012
17. Ning J, Liang SY (2018) Model-driven determination of Johnson-Cook material constants using temperature and force measurements. Int J Adv Manuf Technol 97(1–4):1053–1060. https://doi.org/10.1007/s00170-018-2022-x
18. Ning J, Nguyen V, Huang Y, Hartwig KT, Liang SY (2018) Inverse determination of Johnson–Cook model constants of ultra-fine-grained titanium based on chip formation model and iterative gradient search. Int J Adv Manuf Technol 99(5–8):1131–1140. https://doi.org/10.1007/s00170-018-2508-6

19. Jaspers SP, Dautzenberg JH (2002) Material behaviour in conditions similar to metal cutting: flow stress in the primary shear zone. J Mater Process Technol 122(2–3):322–330. https://doi.org/10.1016/S0924-0136(01)01228-6
20. Adibi-Sedeh AH, Madhavan V, Bahr B (2003) Extension of Oxley's analysis of machining to use different material models. J Manuf Sci Eng 125(4):656–666. https://doi.org/10.1115/1.1617287
21. Lin YC, Chen XM, Liu G (2010) A modified Johnson–Cook model for tensile behaviors of typical high-strength alloy steel. Mater Sci Eng A 527(26):6980–6986. https://doi.org/10.1016/j.msea.2010.07.061
22. Pan Z, Shih DS, Tabei A, Garmestani H, Liang SY (2017) Modeling of Ti-6Al-4V machining force considering material microstructure evolution. Int J Adv Manuf Technol 91(5–8):2673–2680. https://doi.org/10.1007/s00170-016-9964-7
23. Pan Z, Shih DS, Garmestani H, Liang SY (2017) Residual stress prediction for turning of Ti-6Al-4V considering the microstructure evolution. Proc Inst Mech Eng B J Eng Manuf:109–117. https://doi.org/10.1177/0954405417712551
24. Oxley PL, Welsh MJ. (1963). Calculating the shear angle in orthogonal metal cutting from fundamental stress-strain-strain rate properties of the work material. In Proceedings of the Fourth International Conference on Machine Tool Design and Research Conference, 73–86. DOI is unavailable
25. Oxley PLB (1989) The mechanics of machining: an analytical approach to assessing machinability. Ellis Horwood Ltd., England
26. Kalman RE, Bucy RS (1961) New results in linear filtering and prediction theory. J Basic Eng 83(1):95–108. https://doi.org/10.1115/1.3658902
27. Ivester RW, Kennedy M, Davies M, Stevenson R, Thiele J, Furness R, Athavale S (2000) Assessment of machining models: progress report. Mach Sci Technol 4(3):511–538. https://doi.org/10.1080/10940340008945720
28. Aydın M (2016) Cutting temperature analysis considering the improved Oxley's predictive machining theory. J Braz Soc Mech Sci Eng 38(8):2435–2448. https://doi.org/10.1007/s40430-016-0514-x
29. Karpat Y, Özel T (2006) Predictive analytical and thermal modeling of orthogonal cutting process—part I: predictions of tool forces, stresses, and temperature distributions. J Manuf Sci Eng 128(2):435–444. https://doi.org/10.1115/1.2162590
30. Jaspers SP, Dautzenberg JH (2002) Material behaviour in metal cutting: strains, strain rates and temperatures in chip formation. J Mater Process Technol 121(1):123–135. https://doi.org/10.1016/S0924-0136(01)01227-4
31. Mia M, Dhar NR (2016) Response surface and neural network based predictive models of cutting temperature in hard turning. J Adv Res 7(6):1035–1044. https://doi.org/10.1016/j.jare.2016.05.004
32. Özel T, Zeren E. (2005). Finite element modeling of stresses induced by high speed machining with round edge cutting tools. In ASME 2005 International Mechanical Engineering Congress and Exposition, 1279–1287. American Society of Mechanical Engineers. https://doi.org/10.1115/IMECE2005-81046